Band structures in doubly odd ^{130}Pr

R. Ma, E. S. Paul, S. Shi,* C. W. Beausang,† W. F. Piel, Jr., N. Xu, and D. B. Fossan
Physics Department, State University of New York at Stony Brook, Stony Brook, New York 11794

T. Chapuran, D. P. Balamuth, and J. W. Arrison
Physics Department, University of Pennsylvania, Philadelphia, Pennsylvania 19104
(Received 8 December 1987)

Two rotational band structures have been identified in doubly odd ^{130}Pr following the ^{110}Cd(^{28}Si,αp3n)^{130}Pr reaction. One band, having no signature splitting, is believed to be built on the near-prolate $\pi h_{11/2}\otimes\nu g_{7/2}$ configuration. A second band, with a small signature splitting, is built on the triaxial $\pi h_{11/2}\otimes\nu h_{11/2}$ configuration. Systematics of recent results for the doubly odd ^{130,132,134}Pr isotopes are presented.

I. INTRODUCTION

Nuclei in the $A\sim130$ mass region are predicted to be soft[1,2] with respect to γ deformation. It has been established that valence quasiparticles from high-j shells are important in stabilizing the nuclear shape at specific values of γ because of relatively strong shape-driving forces on the γ-soft cores. Shapes (γ values) favored by valence and rotational-aligned quasiparticles from high-j shells are predicted[3] to change significantly as a function of the Fermi surface. In this mass region both the proton and neutron Fermi surfaces lie within the same high-j shell, namely, the $h_{11/2}$ shell. Valence protons from the lower $h_{11/2}$ midshell drive the nucleus towards $\gamma\sim0°$, stabilizing a collective prolate shape, while valence neutrons from the upper $h_{11/2}$ midshell tend to drive the nucleus towards negative values $\gamma\sim-60°$ ($\gamma=-60°$ represents the collective rotation of an oblate shape, the Lund convention[4]).

Recent experiments have shown that, in general, the $\pi h_{11/2}$ yrast bands of odd proton nuclei in this mass region are prolate.[5,6] In contrast, the $\nu h_{11/2}$ yrast bands of odd neutron nuclei possess significant triaxial shapes[7,8] with $\gamma\sim-20°$. In doubly odd nuclei, rotational bands have been established[9–11] that are built on the $\pi h_{11/2}\otimes\nu h_{11/2}$ configuration. In such bands, the shape driving effects of the valence proton and neutron are opposite. The measured signature splitting of these bands implies nonaxial shapes intermediate between those of odd-proton nuclei ($\gamma\sim0°$) and odd-neutron nuclei ($\gamma\sim-20°$). In addition, bands have been observed[9,11] in doubly odd nuclei built on the $\pi h_{11/2}\otimes\nu g_{7/2}$ configuration. Again, the valence neutron from the top of the $g_{7/2}$ shell drives to negative γ, but with less strength than the $h_{11/2}$ neutron. Indeed, the lack of signature splitting in such bands is consistent with near-axial shapes ($\gamma\sim0°$).

The evolution of nuclear properties as a function of neutron number for several Pr isotopes has recently been studied at Stony Brook. The present paper reports on the level structure of ^{130}Pr for which no previous data exist. A comparison with the results[10,11] for the ^{132,134}Pr isotopes is presented.

II. EXPERIMENTAL METHODS AND RESULTS

The high spin states of ^{130}Pr were populated using the ^{110}Cd(^{28}Si,αp3n)^{130}Pr reaction. The silicon beam of energy 160 MeV was accelerated by the tandem-LINAC facility of the Nuclear Structure Laboratory at Stony Brook. An isotopically enriched cadmium target of thickness 2.5 mg/cm^2 was rolled onto a lead backing of thickness 50 mg/cm^2. An array of four Ge detectors, each within a transverse bismuth germanate (BGO) Compton-suppressor,[12] was used to record γ-γ coincidence data. The efficiency of each detector was approximately 25% relative to that for a 7.6 cm$\times$7.6 cm NaI(Tl) detector for 1.3 MeV γ rays. The detectors were positioned at $\pm57°$, and $\pm136°$ with respect to the beam direction, at a distance of 14 cm from the target. Data were recorded event-by-event onto magnetic tapes for subsequent off-line analysis on a VAX 11-780 computer where the coincidence data were used to construct a symmetrized $2k\times2k$ array of E_γ vs E_γ. Background-subtracted spectra were obtained from this array; some typical gated spectra are shown in Fig. 1.

The identification of the observed coincident γ rays with transitions in ^{130}Pr is based on a separate measurement of charged-particle–gamma-ray coincidences using the ^{31}P+^{106}Pd reaction at a bombarding energy of 155 MeV. Evaporated protons and α particles were detected with a phoswich telescope consisting of a 100 μm plastic ΔE detector coupled to a 3 mm thick CaF_2(Eu) E detector. The particle detector, which was mounted at 90° to the beam direction, is identical to those modules used in the University of Pennsylvania 4π array.[13] With this beam and target combination ^{130}Pr is produced by α3n evaporation. Candidate γ rays should thus appear in coincidence with α particles and *not* in coincidence with protons. A portion of the γ spectra observed in coincidence with α particles and protons separately is shown in Fig. 2. Many of the strong γ transitions near the bottom of the cascades shown in the decay scheme of Fig. 3 have the required properties. These observations require the reaction producing these cascades to involve the evaporation of only α particles and neutrons. The number of each can be partially addressed by examining the α particle energy spectra in coincidence with individual candi-

date γ rays and comparing them with corresponding spectra in coincidence with γ rays from known reaction channels. (It is known that the average energies of evaporated particles is, loosely speaking, correlated with the total number of particles emitted.) The results of this comparison, while not completely conclusive, are consistent with the assignment of the observed cascades to the α3n channel.

The constructed level scheme of ^{130}Pr is shown in Fig. 3, where the ordering of the γ rays is based on their intensities obtained from γ-γ coincidence spectra together with systematic properties. Angular correlation information was extracted from the coincidence data. A two-dimensional angular correlation array was created from the data with the $\pm$136° detectors as one axis, and the $\pm$57° detectors as the other. Gated spectra generated from this array were used to obtain directional correlation[14] (DCO) intensity ratios $I_\gamma(136°)/I_\gamma(57°)$. The results of this analysis are presented in Table I. Quadrupole ($E2$) transitions were used as the gating transitions. Empirically, the DCO intensity ratio is greater than 1.0 for stretched quadrupole transitions and less than 0.9 for stretched dipole transitions. The relative intensities of the ^{130}Pr transitions (see Table I) were obtained from the coincidence data, and since these data are averaged over all possible pairs of detectors, any angular correlation effects to these intensities are expected to be small. The intensities have been corrected for internal conversion and detector efficiency, and the values normalized to the 184.8 keV $10^+ \rightarrow 9^+$ transition. The angular correlation data, together with the systematics of Nilsson single-particle levels and comparisons with the neighboring doubly odd nuclei, have been used to assign the spins and multipolarities for the transitions in ^{130}Pr.

The band-head spin and parity of band 2 in Fig. 3 has been tentatively assigned $I^\pi = 8^+$, assuming that the band is based on the positive parity $\pi h_{11/2} \otimes \nu h_{11/2}$ configuration. This assignment is based on a comparison with the ^{132}Pr isotope[11] and other doubly odd nuclei[9,10] in this mass region. Furthermore, perpendicular coupling of the spins of the low-Ω $h_{11/2}$ proton and high-Ω $h_{11/2}$ neutron yield a value $I \sim 8$. The band-head spin and parity of band 1 are taken as 7^-, assuming that the 110.1 keV linking transition is of stretched $E1$ character. The angular correlation ratio for this transition (0.85$\pm$0.17) is consistent with this assignment. Moreover, the γ ray intensity ratio I_γ(89.5 keV)/I_γ(110.1 keV)$\sim$0.5, observed in the spectrum gated by the 184.8 keV transition [Fig. 1(b)] is consistent with an ($M1$,$E1$) assignment for these two transitions. It is expected that the intensities of the 89.5 and 110.1 keV transitions should be approximately equal

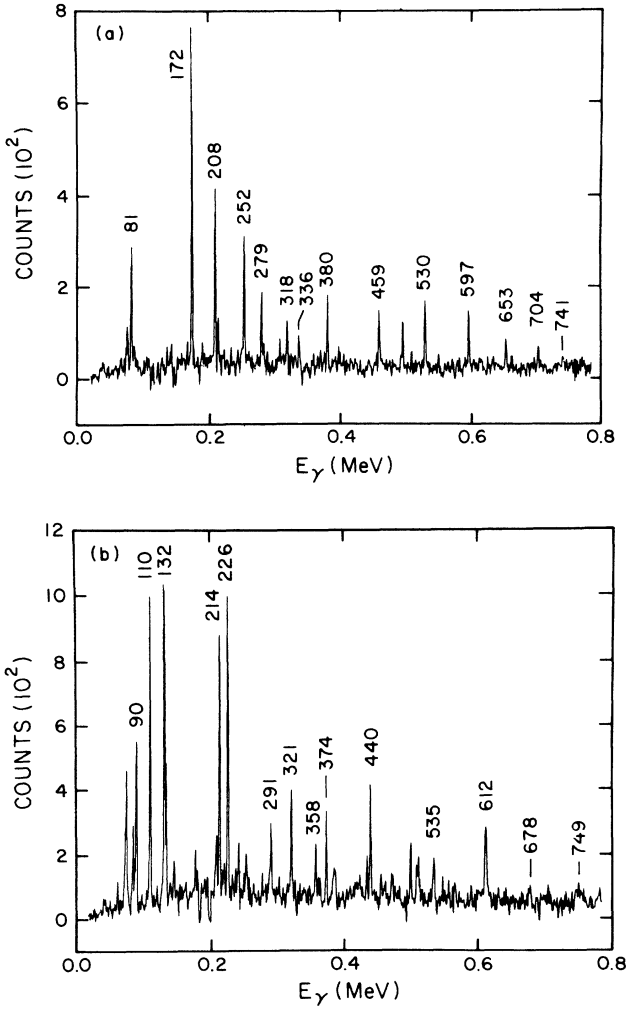

FIG. 1. (a) A background-subtracted spectrum gated on the 123.6 keV transition ($9^- \rightarrow 8^-$) showing transitions in the bands based on the $\pi h_{11/2} \otimes \nu g_{7/2}$ configuration. (b) A background-subtracted spectrum gated on the 184.8 keV transition ($10^+ \rightarrow 9^+$) showing transitions in the bands based on the $\pi h_{11/2} \otimes \nu h_{11/2}$ configuration.

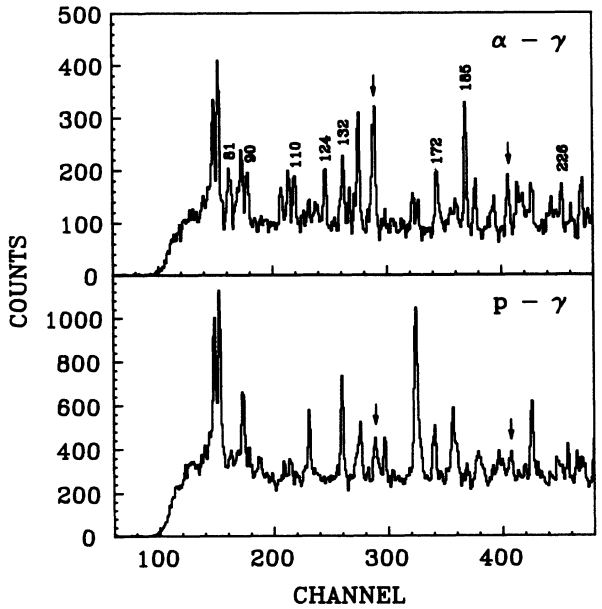

FIG. 2. An α-gated (top) and proton-gated (bottom) γ-ray spectrum from the ^{31}P+^{106}Pd reaction showing transitions (labeled in keV) assigned to ^{130}Pr, the α3n channel. For comparison, known transitions in the αp3n channel are marked with arrows.

since they occur below the gating 184.8 keV transition. The observed intensity ratio of ~ 0.5 is caused by the different internal conversion coefficients for $M1$ and $E1$ transitions. For comparison, the theoretical γ ray intensity ratio for this assignment is ~ 0.4. Band 1 is believed to be built on the negative parity $\pi h_{11/2} \otimes \nu g_{7/2}$ configuration. No rigorous spin and parity measurements have been undertaken for ^{130}Pr.

III. DISCUSSION

A. Experimental alignments and Routhians

Following the procedures of Bengtsson and Frauendorf[15] the alignment (quasiparticle contribution to the spin aligned with the rotation axis)

$$i_x = I_x(\omega) - I_{x,\mathrm{ref}}(\omega) , \tag{1}$$

and Routhian (quasiparticle energy in the rotating frame)

$$e'(\omega) = E'(\omega) - E'_{\mathrm{ref}}(\omega) , \tag{2}$$

have been extracted for the two bands in ^{130}Pr; the results are presented as a function of rotational frequency in Fig. 4. In the preceding equations I_x is the total angular momentum component on the rotational axis given semiclassically as

$$I_x = [(I+\tfrac{1}{2})^2 - \langle K \rangle^2]^{1/2} , \tag{3}$$

while $I_{x,\mathrm{ref}}$ corresponds to a reference configuration evaluated with a frequency-dependent moment of inertia (the Harris expression[16]) $\mathcal{J}_{\mathrm{ref}} = \mathcal{J}_0 + \omega^2 \mathcal{J}_1$. The parameters in the reference were obtained by fitting the expression

$$I_x = \omega \mathcal{J}_{\mathrm{ref}} + i_x = \omega(\mathcal{J}_0 + \omega^2 \mathcal{J}_1) + i_x \tag{4}$$

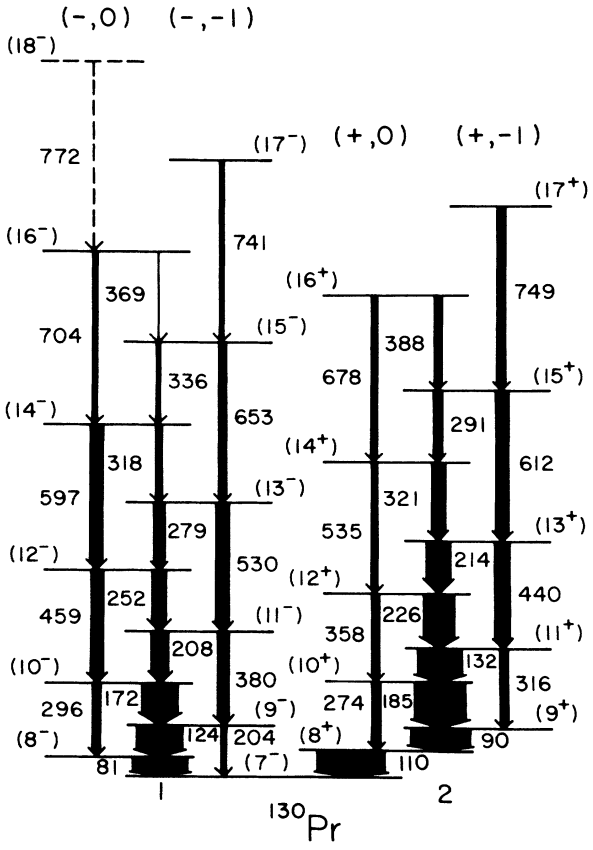

FIG. 3. Proposed level scheme of ^{130}Pr constructed from this work. The transition energies are given in keV and their intensities are indicated by the width of the arrows. Lower limits are shown for the intensities of the low energy 81, 90, and 110 keV transitions. The bands are labeled by parity and signature quantum numbers (π,α).

TABLE I. Energies, relative intensities, and angular correlation data for transitions in doubly odd ^{130}Pr.

E_γ (keV)[a]	Intensity[b]	DCO ratio[c]	Assignment[d]
81.1	>108[e]	0.76(21)	$8^- \rightarrow 7^-$
89.5	>116[e]		$9^+ \rightarrow 8^+$
110.1	>132[e]	0.85(17)	$8^+ \rightarrow 7^-$
123.6	89.5	0.86(24)	$9^- \rightarrow 8^-$
131.5	87.7		$11^+ \rightarrow 10^+$
172.3	68.3	0.63(10)	$10^- \rightarrow 9^-$
184.8	$\equiv 100$	0.68(8)	$10^+ \rightarrow 9^+$
207.6	32.0	0.40(12)	$11^- \rightarrow 10^-$
213.7	48.8		$13^+ \rightarrow 12^+$
226.3	58.4	0.64(14)	$12^+ \rightarrow 11^+$
252.0	29.0	0.67(10)	$12^- \rightarrow 11^-$
274.3	17.0		$10^+ \rightarrow 8^+$
278.6	19.1	0.60(13)	$13^- \rightarrow 12^-$
290.9	15.8	0.60(20)	$15^+ \rightarrow 14^+$
295.7	17.8(3.3)	0.98(10)	$10^- \rightarrow 8^-$
315.6	15.5(3.0)	1.24(51)	$11^+ \rightarrow 9^+$
318.1	13.0		$14^- \rightarrow 13^-$
321.2	26.4	0.87(23)	$14^+ \rightarrow 13^+$
335.7	5.6(1.4)		$15^- \rightarrow 14^-$
358.1	13.8	1.09(32)	$12^+ \rightarrow 10^+$
369.0	<5		$16^- \rightarrow 15^-$
379.5	20.3	1.36(37)	$11^- \rightarrow 9^-$
387.5	12.2(1.9)		$16^+ \rightarrow 15^+$
440.0	28.1	1.06(32)	$13^+ \rightarrow 11^+$
459.3	23.7	1.08(18)	$12^- \rightarrow 10^-$
530.1	25.2	1.36(30)	$13^- \rightarrow 11^-$
534.9	12.6(1.9)		$14^+ \rightarrow 12^+$
596.9	23.2		$14^- \rightarrow 12^-$
612.3	21.0		$15^+ \rightarrow 13^+$
653.2	12.1(1.8)	1.02(28)	$15^- \rightarrow 13^-$
678.0	13.2		$16^+ \rightarrow 14^+$
703.6	10.7(1.8)		$16^- \rightarrow 14^-$
741.0	6.6(1.7)		$17^- \rightarrow 15^-$
748.6	16.8(2.4)		$17^+ \rightarrow 15^+$
772	<5		$18^- \rightarrow 16^-$

[a]Energies of the transitions are accurate to ± 0.2 keV.
[b]The transition intensities are normalized to the 184.8 keV transition ($\equiv 100$). Except where stated, the errors are less than 10%.
[c]Angular intensity ratios $I_\gamma(136°)/I_\gamma(57°)$ were obtained using quadrupole transitions as the gating transitions.
[d]No rigorous spin and parity measurements have been made for ^{130}Pr. The assignments are based on the DCO ratios, systematic properties, and theoretical considerations.
[e]Lower limit for the intensity obtained by summing the intensities of observed feeding transitions.

to the bands in ^{130}Pr. The values obtained for the $\pi h_{11/2}\otimes\nu g_{7/2}$ band (band 1) were $\mathcal{J}_0=19.4\hbar^2$ MeV^{-1} and $\mathcal{J}_1=57.2\hbar^4$ MeV^{-3}, while parameter values $\mathcal{J}_0=19.4\hbar^2$ MeV^{-1} and $\mathcal{J}_1=29.3\hbar^4$ MeV^{-3} were obtained for the $\pi h_{11/2}\otimes\nu h_{11/2}$ band (band 2). A value $\langle K\rangle=3$ was used for each band. The results will be discussed in more detail in the following subsections.

B. Band structures in ^{130}Pr

In doubly odd nuclei, two-quasiparticle states are formed by adding an odd proton (Ω_p) and an odd neutron (Ω_n) to a deformed even-even core. According to the Gallagher-Moszkowski coupling rule,[17] the particles are coupled such that their spins align parallel. A second energetically favorable situation occurs if their orbital angular momenta align antiparallel. For the case of $\Omega_p=\Lambda_p\pm\frac{1}{2}$, $\Omega_n=\Lambda_n\mp\frac{1}{2}$, both requirements are fulfilled if $K=|\Omega_p-\Omega_n|$, which is the "strong" coupling rule. The "weak" coupling rule $K=|\Omega_p+\Omega_n|$ occurs when $\Omega_p=\Lambda_p\pm\frac{1}{2}$, $\Omega_n=\Lambda_n\pm\frac{1}{2}$, because only one condition (spins parallel) is fulfilled. In ^{130}Pr, two bands are formed by the weak coupling of a low-Ω $h_{11/2}$ proton orbital to two different high-Ω neutron orbitals. The coupled neutron orbitals allow for the observation of both signature components of the rotational bands.

The first available $h_{11/2}$ orbital for the odd proton is the $[541]\frac{3}{2}^-$ Nilsson orbital. The available neutron orbitals near the Fermi surface are the $g_{7/2}[402]\frac{5}{2}^+$ and $h_{11/2}[523]\frac{7}{2}^-$ orbitals. Coupling these two neutron orbitals to the $h_{11/2}$ proton leads to a negative parity band built on the $\pi h_{11/2}\otimes\nu g_{7/2}$ configuration and a positive parity band built on the $\pi h_{11/2}\otimes\nu h_{11/2}$ configuration. The lowest energy configurations have $K^\pi=4^-$ and 5^+, respectively, according to the weak coupling rule. However, nonaxial shapes and rotation can mix states of good K to produce an effective value $\langle K\rangle$. Band 1 of Fig. 3 has been identified with the negative parity $\pi h_{11/2}\otimes\nu g_{7/2}$ configuration, while band 2 has been identified with the $\pi h_{11/2}\otimes\nu h_{11/2}$ configuration.

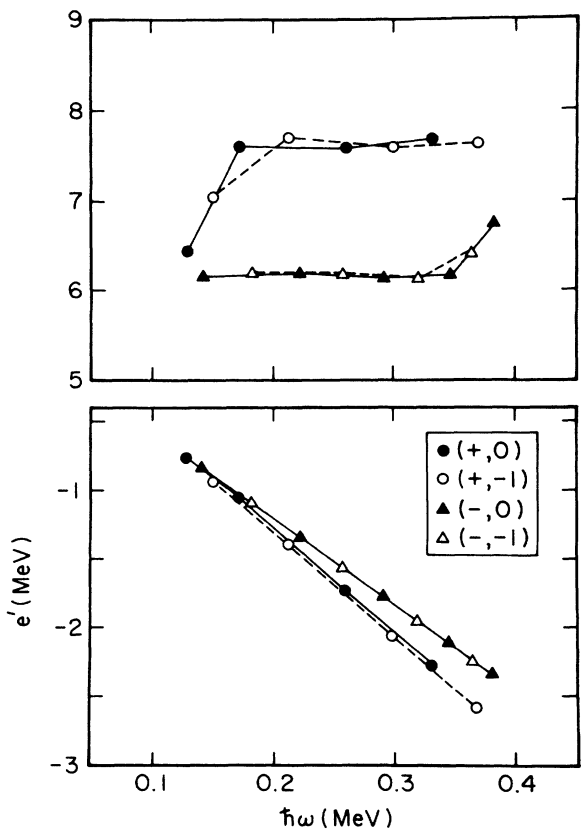

FIG. 4. Experimental alignments i_x in units of $\hbar$ (a) and Routhians (b) for the positive parity band (circles) and negative parity band (triangles) as a function of rotational frequency.

The experimental alignments and Routhians for the two bands in ^{130}Pr are shown in Fig. 4 using the reduced value $\langle K\rangle=3$ for both bands. These values gave the best fit to experimental $B(M1)/B(E2)$ ratios as discussed herein. For the $\pi h_{11/2}\otimes\nu g_{7/2}$ band, the experimental alignment is constant at about $6.1\hbar$ below a rotational frequency $\hbar\omega=0.38$ MeV. For the $\pi h_{11/2}\otimes\nu h_{11/2}$ band, an alignment $i_x\sim7.5\hbar$ is extracted which is close to the sum of the alignments observed in $h_{11/2}$ bands of neighboring odd-proton ($\sim5\hbar$) and odd-neutron ($\sim2\hbar$) nuclei. Below a frequency $\hbar\omega=0.2$ MeV, the alignment of the $\pi h_{11/2}\otimes\nu h_{11/2}$ band drops sharply by $1\hbar$ and may be caused by a recoupling of the particles to produce a larger $\langle K\rangle$ value.

No signature splitting is observed between the odd-spin and even-spin band members of the $\pi h_{11/2}\otimes\nu g_{7/2}$ band (band 1), while a modest signature splitting $\Delta e'=33$ keV is seen for the $\pi h_{11/2}\otimes\nu h_{11/2}$ band (band 2). The lack of band crossings observed below a rotational frequency $\hbar\omega=0.38$ MeV in each band confirms that the odd proton occupies an $h_{11/2}$ orbital, thus blocking the low frequency ($\hbar\omega_c\sim0.3$ MeV) decoupling of the first pair of valence $h_{11/2}$ quasiprotons.

C. Cranked shell model calculations

Cranked shell calculations as a function of the γ deformation have been performed for ^{130}Pr using the formalism of Frauendorf and May.[18] These calculations predict a nuclear shape $\gamma\sim-5°$ for the $\pi h_{11/2}\otimes\nu g_{7/2}$ band with no signature splitting. For the $\pi h_{11/2}\otimes\nu h_{11/2}$ band, a shape of $\gamma\sim-10°$ is predicted together with a small signature splitting $\Delta e'\sim50$ keV. These predictions are consistent with the experimental observations and thus strengthen the assigned configurations. Similar calculations have been presented in more detail for the doubly odd nuclei ^{130}La and ^{132}Pr in Refs. 9 and 11, respectively.

D. Electromagnetic properties: Experimental $B(M1)/B(E2)$ ratios

Relative reduced transition rates

$$B(M1;I\rightarrow I-1)/B(E2;I\rightarrow I-2)$$

can be readily extracted from the intensities of the observed $\Delta I=2$ and $\Delta I=1$ transitions using the expression

$$\frac{B(M1;I\rightarrow I-1)}{B(E2;I\rightarrow I-2)}=0.693\frac{I_\gamma(M1)}{I_\gamma(E2)}\frac{E_\gamma^5(E2)}{E_\gamma^3(M1)}\ . \quad (5)$$

This expression assumes the $E2/M1$ mixing ratio δ for the $\Delta I=1$ transitions is zero, which is justified since the ratios are proportional to $(1+\delta^2)^{-1}$ with δ^2 being typically only a few percent.

Experimental ratios for the bands built on the $\pi h_{11/2}\otimes\nu g_{7/2}$ and $\pi h_{11/2}\otimes\nu h_{11/2}$ configurations in ^{130}Pr are presented in Fig. 5. The solid and dashed lines are predicted values for these configurations calculated using the geometrical model of Dönau and Frauendorf,[19] in which a coupled neutron (large Ω_n) and a decoupled proton (small Ω_p) are considered. The best fit to the experimental data was obtained using a reduced $\langle K\rangle=3$ for both bands. Although the expected value for the two configurations are $K^\pi=4^-$ and $K^\pi=5^+$, respectively, both rotation and the nonaxial shapes could lower the effective $\langle K\rangle$ and, hence, also the $B(M1)/B(E2)$ ratios which are proportional to $\langle K\rangle^2$. The value $\langle K\rangle=3$ was also used in extracting the experimental Routhians and alignments for both bands. The high data point for $I^\pi=11^+$ occurs exactly when the alignment of the $\pi h_{11/2}\otimes\nu h_{11/2}$ falls sharply, as shown in Fig. 4.

E. Comparison with the ^{132,134}Pr isotopes

The doubly odd isotopes ^{132,134}Pr have recently been studied at Stony Brook.[10,11] The systematics of the level excitation energies in a series of isotopes is a useful way to test the consistency of the spin assignment and to compare the systematic properties of nuclei. The level structures are plotted in Fig. 6 for the $\alpha=0$ and $\alpha=-1$ signatures in the series of ^{130,132,134}Pr isotopes. The band spacings of the isotopes decrease towards the lighter isotopes.

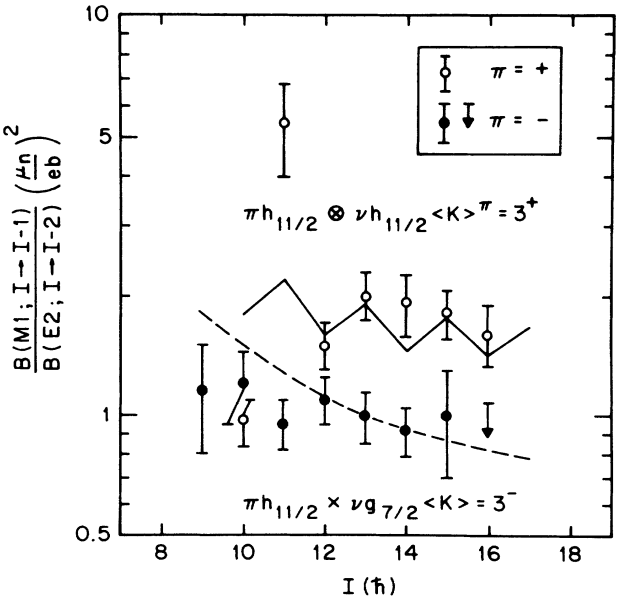

FIG. 5. Experimental values of $B(M1)/B(E2)$ ratios for the positive parity band (open circles) and negative parity band (solid circles); theoretical estimates are also presented for the positive parity band (solid line) and negative parity band (dashed line).

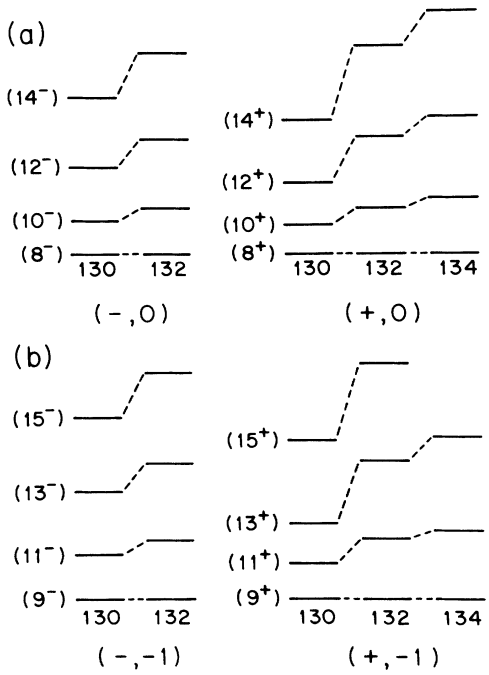

FIG. 6. (a) Energy systematics of the nuclei ^{130,132,134}Pr for the $\alpha=0$ signatures. The level $I=8$ was used as the reference energy. (b) Energy systematics of the nuclei ^{130,132,134}Pr for the $\alpha=-1$ signatures. The level $I=9$ was used as the reference energy.

This indicates the effect of an increasing quadrupole deformation for the more neutron-deficient isotopes.

Rotational bands built on the $\pi h_{11/2}\otimes\nu h_{11/2}$ structure have been observed[10,11] in the ^{130,132,134}Pr isotopes in addition to other doubly odd nuclei[9,20–22] in this mass region. A comparison of the signature splittings observed in such bands of some lanthanum and praseodymium isotopes is made in Table II. As can be seen, the value obtained for ^{130}Pr is smaller than the values for the other nuclei. The $\pi h_{11/2}\otimes\nu g_{7/2}$ structure has also been observed[11,9] in ^{132}Pr and ^{130}La. In each case, no signature splitting is observed in these bands.

The $B(M1)/B(E2)$ ratios extracted for the $\pi h_{11/2}\otimes\nu h_{11/2}$ band in ^{130}Pr are only $\sim 50\%$ of the values observed for the corresponding band in the heavier ^{132}Pr isotope. This difference may reflect a different $\langle K\rangle$ value for the bands in each nucleus.

TABLE II. A comparison of experimental signature splittings extracted for $\pi h_{11/2}\otimes\nu h_{11/2}$ bands in several doubly odd nuclei. The values were obtained at a rotational frequency $\hbar\omega=0.3$ MeV but are essentially constant to the highest observed frequencies. The references for the data are also shown.

Nucleus	Data reference	Signature splitting $\Delta e'$ (keV)
^{128}La	20	38±3
^{130}La	9	42±3
^{130}Pr		33±3
^{132}Pr	11	49±3
^{134}Pr	10	45±3

IV. CONCLUSIONS

Two collective rotational bands have been established in ^{130}Pr, both consisting of strong $\Delta I=1$ transitions with weaker crossover $\Delta I=2$ transitions. One band, with no signature splitting, is believed to be built on the negative parity $\pi h_{11/2}\otimes\nu g_{7/2}$ configuration which stabilizes a near-prolate nuclear shape. A second band, with a small signature splitting $\Delta e'\sim 35$ keV, is believed to be built on the positive parity $\pi h_{11/2}\otimes\nu h_{11/2}$ configuration with a slightly triaxial shape $\gamma\sim -10°$. The shapes of doubly odd nuclei in mass region are, in general, intermediate between those of neighboring odd-Z nuclei ($\gamma\sim 0°$) and odd-N nuclei ($\gamma\sim -20°$). It is the competition between the opposing γ-driving forces of the odd lower-midshell proton and the odd upper-midshell neutron which stabilize these nuclear shapes.

ACKNOWLEDGMENTS

This work was supported in part by the National Science Foundation. One of us (S.S.) was supported by a K. K. Leung Fellowship through the Committee of Educational Exchange with China.

*Present address: Institute of Nuclear Research, Shanghai, China.

†Present address: Lawrence Berkeley Laboratory, University of California, Berkeley, CA 94720.

[1]I. Ragnarsson, A. Sobiczewski, R. K. Sheline, S. E. Larsson, and B. Nerlo-Pomorska, Nucl. Phys. **A233**, 329 (1974).

[2]Y. S. Chen, S. Frauendorf, and G. A. Leander, Phys. Rev. C **28**, 2437 (1983).

[3]G. A. Leander, S. Frauendorf, and F. R. May, in *Proceedings of the Conference on High Angular Momentum Properties of Nuclei, Oak Ridge, 1982,* edited by N. R. Johnson (Harwood-Academic, New York, 1983), p. 281.

[4]G. Andersson, S. E. Larsson, G. Leander, P. Möller, S. G. Nilsson, I. Ragnarsson, S. Åberg, R. Bengtsson, J. Dudek, B. Nerlo-Pomorska, K. Pomorski, and Z. Szymański, Nucl. Phys. **A268**, 205 (1976).

[5]L. Hildingsson, C. W. Beausang, D. B. Fossan, and W. F. Piel, Jr., Phys. Rev. C **33**, 2200 (1986).

[6]C. W. Beausang, L. Hildingsson, E. S. Paul, W. F. Piel, Jr., P. K. Weng, N. Xu, and D. B. Fossan, Phys. Rev. C **36**, 602 (1987).

[7]R. Aryaeinejad, D. J. G. Love, A. H. Nelson, P. J. Nolan, P. J. Smith, D. M. Todd, and P. J. Twin, J. Phys. G **10**, 955 (1984).

[8]W. F. Piel, Jr., C. W. Beausang, D. B. Fossan, L. Hildingsson, and E. S. Paul, Phys. Rev. C **35**, 959 (1987).

[9]E. S. Paul, C. W. Beausang, D. B. Fossan, R. Ma, W. F. Piel, Jr., N. Xu, and L. Hildingsson, Phys. Rev. C **36**, 1853 (1987).

[10]C. W. Beausang, L. Hildingsson, E. S. Paul, W. F. Piel, Jr., P. K. Weng, N. Xu, and D. B. Fossan, Phys. Rev. C **36**, 1810 (1987).

[11]S. Shi, C. W. Beausang, D. B. Fossan, R. Ma, E. S. Paul, W. F. Piel, Jr., N. Xu, L. Hildingsson, and A. J. Kreiner, Bull. Am. Phys. Soc. **32**, 1562 (1987); and submitted to Phys. Rev. C.

[12]L. Hildingsson, C. W. Beausang, D. B. Fossan, W. F. Piel, Jr., A. P. Byrne, and G. D. Dracoulis, Nucl. Instrum. Methods **A252**, 91 (1986).

[13]T. Chapuran, D. P. Balamuth, H. S. Sozuer, J. Görres, and J. Arrison, Bull. Am. Phys. Soc. **30**, 1250 (1985); T. Chapuran, D. P. Balamuth, J. W. Arrison, and J. Görres (unpublished).

[14]K. S. Krane, R. M. Steffen, and R. M. Wheeler, Nucl. Data Tables **A11**, 351 (1973).

[15]R. Bengtsson and S. Frauendorf, Nucl. Phys. **A327**, 139 (1979).

[16]S. M. Harris, Phys. Rev. **138**, B509 (1965).

[17]C. J. Gallagher and S. A. Moskowski, Phys. Rev. **111**, 1282 (1958).

[18]S. Frauendorf and F. R. May, Phys. Lett. **125B**, 245 (1983).

[19]F. Dönau and S. Frauendorf, in *Proceedings of the Conference on High Angular Momentum Properties of Nuclei, Oak Ridge, 1982,* edited by N. R. Johnson (Harwood-Academic, New York, 1983), p. 143; and F. Dönau, Niels Bohr Institute–Zentralinstitut für Kernforschung Report 85-36, 1985.

[20]M. A. Quader, C. W. Beausang, P. Chowdhury, U. Garg, and D. B. Fossan, Phys. Rev. C **33**, 1109 (1986).

[21]P. J. Nolan, R. Aryaeinejad, P. J. Bishop, M. J. Godfrey, A. Kirwan, D. J. G. Love, A. H. Nelson, D. J. Thornley, and D. J. Unwin, J. Phys. G **13**, 1555 (1987).

[22]C. W. Beausang, P. K. Weng, E. S. Paul, W. F. Piel, Jr., N. Xu, and D. B. Fossan, Bull. Am. Phys. Soc. **31**, 1212 (1986).